

Article

Studies on the Reactions of Biapenem with VIM Metallo β -Lactamases and the Serine β -Lactamase KPC-2

Anka Lucic ¹, Tika R. Malla ¹, Karina Calvopiña ¹, Catherine L. Tooke ², Jürgen Brem ¹ , Michael A. McDonough ¹, James Spencer ² and Christopher J. Schofield ^{1,*} 

- ¹ Chemistry Research Laboratory, The Department of Chemistry and the Ineos Oxford Institute for Antimicrobial Research, University of Oxford, Oxford OX1 3TA, UK; anka.lucic@strubi.ox.ac.uk (A.L.); tika.malla@chem.ox.ac.uk (T.R.M.); karina.calvopinapia@chem.ox.ac.uk (K.C.); jurgen.brem@chem.ox.ac.uk (J.B.); michael.mcdonough@chem.ox.ac.uk (M.A.M.)
- ² Biomedical Sciences Building, School of Cellular and Molecular Medicine, Faculty of Life Sciences, University of Bristol, University Walk, Bristol BS8 1TD, UK; ct12425@bristol.ac.uk (C.L.T.); jim.spencer@bristol.ac.uk (J.S.)
- * Correspondence: christopher.schofield@chem.ox.ac.uk

Abstract: Carbapenems are important antibacterials and are both substrates and inhibitors of some β -lactamases. We report studies on the reaction of the unusual carbapenem biapenem, with the subclass B1 metallo- β -lactamases VIM-1 and VIM-2 and the class A serine- β -lactamase KPC-2. X-ray diffraction studies with VIM-2 crystals treated with biapenem reveal the opening of the β -lactam ring to form a mixture of the (2*S*)-imine and enamine complexed at the active site. NMR studies on the reactions of biapenem with VIM-1, VIM-2, and KPC-2 reveal the formation of hydrolysed enamine and (2*R*)- and (2*S*)-imine products. The combined results support the proposal that SBL/MBL-mediated carbapenem hydrolysis results in a mixture of tautomerizing enamine and (2*R*)- and (2*S*)-imine products, with the thermodynamically favoured (2*S*)-imine being the major observed species over a relatively long-time scale. The results suggest that prolonging the lifetimes of β -lactamase carbapenem complexes by optimising tautomerisation of the nascently formed enamine to the (2*R*)-imine and likely more stable (2*S*)-imine tautomer is of interest in developing improved carbapenems.

Keywords: carbapenems; antimicrobial resistance; metallo- β -lactamases; serine- β -lactamases; biapenem



Citation: Lucic, A.; Malla, T.R.; Calvopiña, K.; Tooke, C.L.; Brem, J.; McDonough, M.A.; Spencer, J.; Schofield, C.J. Studies on the Reactions of Biapenem with VIM Metallo β -Lactamases and the Serine β -Lactamase KPC-2. *Antibiotics* **2022**, *11*, 396. <https://doi.org/10.3390/antibiotics11030396>

Academic Editor: Krisztina M. Papp-Wallace

Received: 25 January 2022

Accepted: 9 March 2022

Published: 16 March 2022

Publisher's Note: MDPI stays neutral with regard to jurisdictional claims in published maps and institutional affiliations.



Copyright: © 2022 by the authors. Licensee MDPI, Basel, Switzerland. This article is an open access article distributed under the terms and conditions of the Creative Commons Attribution (CC BY) license (<https://creativecommons.org/licenses/by/4.0/>).

1. Introduction

β -Lactam-containing drugs are the most clinically important antibacterial class [1], though their use is increasingly impaired by resistance due to nucleophilic serine- β -lactamases (SBLs, Ambler classes A, C and D) and zinc-dependent metallo- β -lactamases (MBLs, Ambler class B) (Figure 1) [2–4]. Carbapenems were once considered antibiotics of ‘last resort’, in part because they are resistant to hydrolysis by some SBLs [1]. However, the increasingly widespread use of carbapenems is correlated with an increase in extended-spectrum SBLs (ESBLs) in both Gram-positive and Gram-negative bacteria [5]. The role of MBLs, such as the Verona integron MBLs, which often efficiently hydrolyse carbapenems, in antimicrobial resistance is also rapidly growing and is now endemic in some regions [6].

The stability of the complexes formed by β -lactams with SBLs/MBLs is an important factor in determining their susceptibility to β -lactamases and hence efficacy. The ability of carbapenems to form relatively stable complexes both with their transpeptidase targets and certain SBLs has contributed to their greater efficacy compared to other β -lactams against some resistant strains. However, there is incomplete knowledge of the molecular factors involved in determining enzyme-carbapenem complex stabilities, as exemplified by the recent observation that carbapenems react with Class D SBLs to produce β -lactones in addition to the established enamine and imine hydrolysed products (Figure 1) [7,8].

Studies on the products of carbapenem hydrolysis by several MBLs and SBLs have led to the proposal that, at least in some cases, during efficient catalysis the major nascent product is in the enamine tautomeric form, which undergoes isomerisation to give the (2*R*)- and (2*S*)-C2 imines (Figure 1) [8–11].

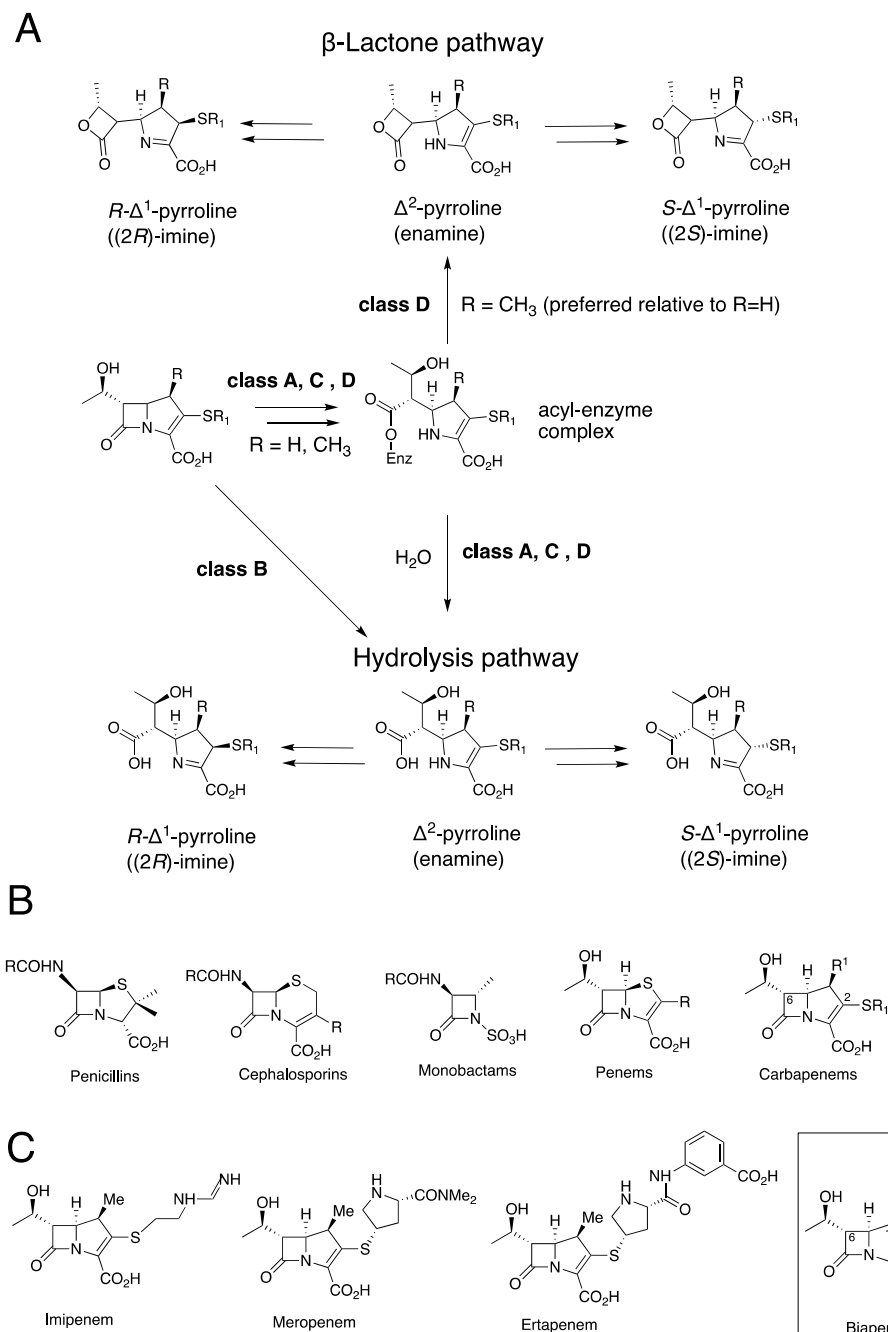


Figure 1. Carbapenem hydrolysis by β -lactamases. **(A)** It is proposed that SBLs and MBLs hydrolyse carbapenems to produce an enamine (Δ^2 -pyrroline), which during efficient catalysis in solution isomerises to give (2*R*)- and (2*S*)- Δ^1 -imine products. Both enamine and (2*S*)- and (2*R*)-imine carbapenem-derived ligands have been observed by crystallography at MBL/SBL/transpeptidase active sites. Lactones can also be formed, at least, in the case of class D SBLs. **(B)** Classes of clinically used β -lactam antibiotics (for carbapenems $R^1 = \text{H}$ or Me). **(C)** Examples of clinically used carbapenems; note the unusual positively charged bicyclic bicyclotriazolium C2 side chain of biapenem.

The intravenously administered carbapenem biapenem has a broad spectrum of activity and is used to treat serious infections [12–14]. Biapenem is reported to have less adverse side effects than other carbapenems and does not need to be administered with a dihydropeptidase 1 inhibitor [13]. Biapenem is an inhibitor of some SBLs but is subject to MBL hydrolysis [12–14]. Since biapenem has the same C6 hydroxyethyl side chain as other carbapenems, its distinctive properties must be due to the presence of its unusual positively charged ‘bicyclotriazolium’ sulfur-linked C2 bicyclic ring system (Figure 1) [12–14]. The unusual C2 side chain of biapenem compared to the more typical C2 side chains of carbapenems such as meropenem makes it of particular interest with respect to defining its tautomeric enamine and imine product profile.

Here, we report studies on the reactions of biapenem with the clinically important VIM-1, VIM-2, and KPC-2 β -lactamases using NMR spectroscopy and, in the case of VIM-2, X-ray crystallographic analysis. After the pioneering identification of the first Verona integron MBL (VIM) in 1996, multiple VIM variants have been observed in Gram-negative bacteria, including in *Klebsiella* and *Enterobacteriaceae* [15,16]. The VIM MBLs are broad-spectrum β -lactamases that catalyse the hydrolysis of penicillins, cephalosporins, and carbapenems, but not monobactams [17–20] (Figure 1C). VIMs have the typical $\alpha\beta/\beta\alpha$ MBL fold and are di-zinc utilising B1 subfamily MBLs [17,19,20]. The *Klebsiella pneumoniae* carbapenemase 2 (KPC-2) is a Class A SBL of increasing clinical importance and has broad-spectrum activity, including with respect to the particularly efficient hydrolysis of carbapenems [21,22].

2. Results

We initially investigated how biapenem reacts with VIM-1, VIM-2, and KPC-2 using ^1H NMR (600 MHz) spectroscopy. In all three cases, enamine and both (2*R*)-imine and (2*S*)-imine products were observed, as evidenced by the analysis of the methyl group resonances (C6 hydroxyethyl methyl and C1 methyl groups) in the high-field region (0.8–1.3 ppm) of the ^1H NMR spectrum. The major product observed was the (2*S*)-imine, consistent with previous work indicating that this is the thermodynamically favoured species of the three observed major tautomeric products. [7–9,20]. Lower levels of the (2*R*)-imine and enamine products were observed, along with low levels of at least one unassigned product with methyl group resonances at ~1.00 and 1.02 ppm (Figures 2 and S1–S4, Table S1). No evidence for the formation of lactone products was accrued, contrasting with the results of reaction of carbapenems with class D SBLs, but consistent with prior work on the reactions of carbapenems with MBLs (Figure 1), [7–9,20]. Overall, our NMR results support the proposal of the (2*S*)-imine as the major product (on the timescale of the NMR assays), though they do not preclude the possibility that the enamine or (2*R*)-imine are nascent products.

Crystal structures have been reported for biapenem-derived complexes with the class B2 MBL CphA and certain transpeptidases [23–25]. However, there is no reported structure for biapenem with a representative of the most clinically relevant class B1 MBLs. Thus, we performed studies to investigate how biapenem interacts with the B1 MBL Verona integron metallo β -lactamase (VIM-2), on which studies with inhibitors have previously been carried out [26,27]. Crystals of recombinant VIM-2 were produced as previously described [20,26] and were soaked with a 50 mM solution of biapenem for 1, 5, 10, and 30 min. A diffraction dataset with a crystal soaked in biapenem for 10 min was obtained with the Diamond Light Source at a 1.3 Å resolution (space group *I*222 with one molecule in the asymmetric unit) (Figure S5, Table S2). Due to low completeness in the high-resolution shell, the resolution for data processing was cut to 1.5 Å.

Analysis of the electron density at the VIM-2 active site led to trial refinements with either the (2*S*)-imine, the (2*R*)-imine or the enamine (independently), the two imines together at 50% occupancy, or the enamine with either the (2*S*)- or (2*R*)-imine at 50% occupancy (Figures 3 and 4). The best fit was obtained with the (2*S*)-imine and the enamine at 50% occupancy. Note that the occupancy level should be regarded as an estimation and we cannot rule out low levels of the presence of the (2*R*)-imine and other ligands; in the

NMR studies, there were some unassigned peaks, consistent with minor product formation (Figures S1 and S2).

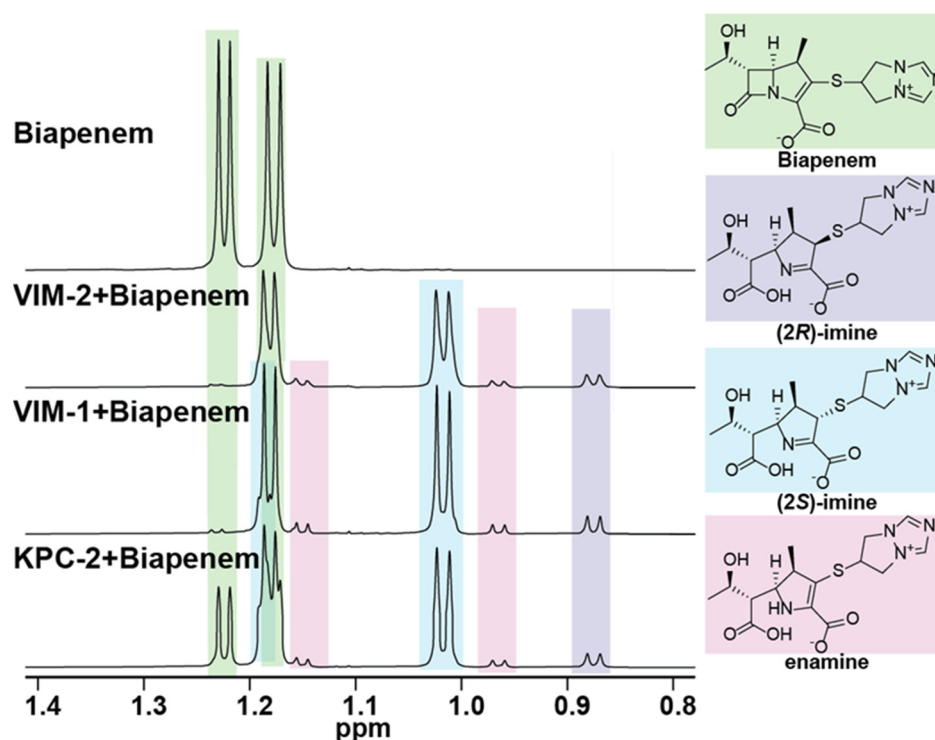


Figure 2. High-field regions of ^1H NMR spectra (600 MHz) for reaction of biapenem with the MBLs VIM-1 or VIM-2, or the SBL KPC-2. Biapenem (5 mM, green) was treated with the purified β -lactamase (280 nM, 30 min) in 50 mM of sodium phosphate at pH 7.6 (with 10% *v/v* D_2O). Formation of enamine (pink) and (2*R*)-imine and (2*S*)-imine (purple and blue, respectively) products was observed in all three cases. Time-course analyses imply the (2*S*)-imine is the major and ‘thermodynamic’ product (Figures S1–S4). The slowest rate of biapenem turnover was observed with KPC-2 (Figure S1), with increasing rates observed for VIM-1 (Figure S2), and VIM-2 (Figure S3).

The apparent electron density for the bicyclic side chains of both the (2*S*)-imine and the enamine ligands was weak, likely due to the lack of protein contacts causing conformational mobility (Figure 3). In general, the interactions made by both the enamine and (2*S*)-imine are analogous to those observed in other VIM-1: carbapenem-derived structures [19], i.e., in both cases the newly formed β -lactam derived carboxylates displace the water/hydroxide ion bridging the two zinc ions, and the C3 carboxylate is positioned to interact with the Arg228 sidechain (Figures S6 and S7). An increase of 0.8 Å in the distance between the two active site zinc ions (4.3 Å) compared to the unliganded structure was also observed, as previously reported in MBL carbapenem and faropenem derived complexes [19,20].

Notably, the thioether of the C2 biapenem-derived sidechain adopts different conformations for the enamine and the (2*S*)-imine ligands, with the sulfur being positioned close to the primary amide of Asn233 in the case of the enamine, but not the (2*S*)-imine (Figures 4 and S6). The C6 hydroxyethyl group is positioned similarly for both the enamine and (2*S*)-imine ligands, in a manner similar to that observed in previous VIM-2 carbapenem/faropenem-derived complexes (Figure S7) [19,20].

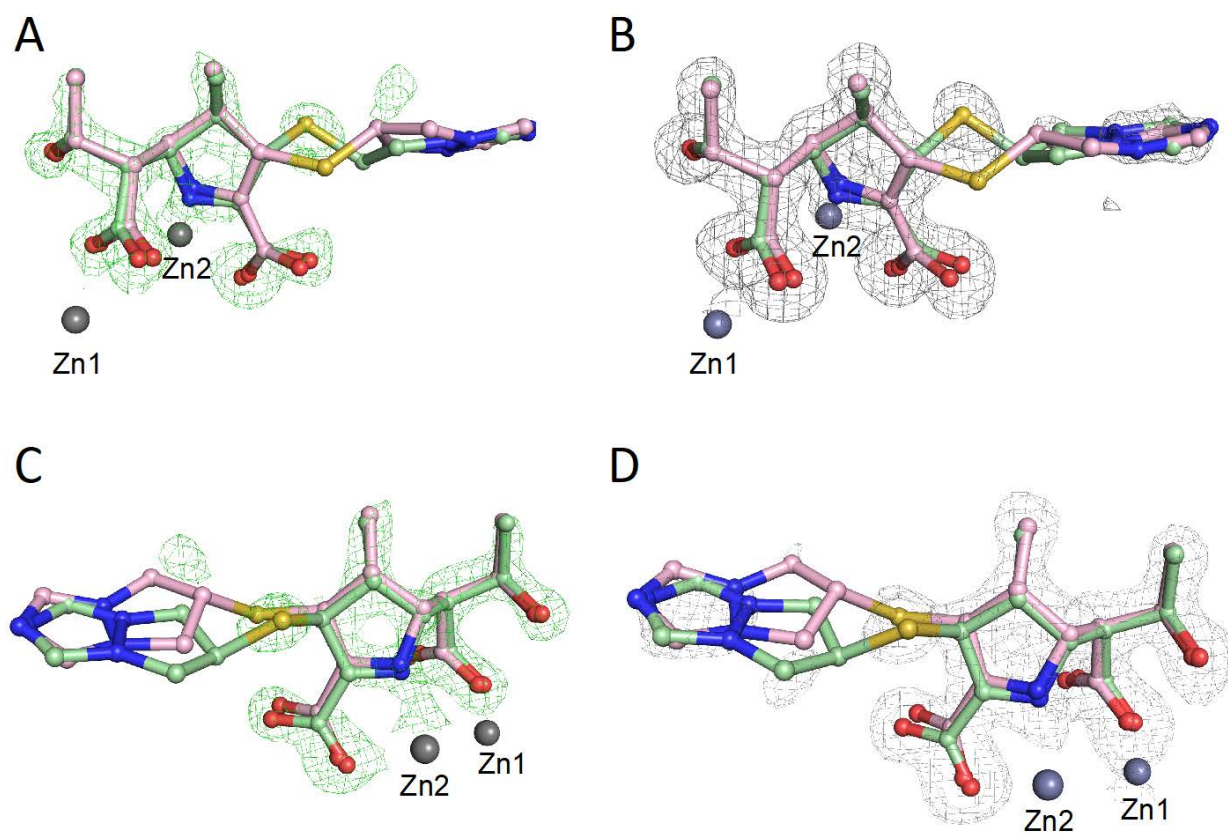


Figure 3. Electron density maps for biapenem-derived products in complex with VIM-2. (2*S*)-Imine: pale green balls and sticks; enamine: pink balls and sticks. (A,C) show an OMIT map (green mesh) of mFo-DFc contoured to 3σ (PDB: 6Y6J). (B,D) show the 2mFo-DFc difference map in grey mesh, contoured to 1σ . Note the weak density for the biapenem-derived bicyclotriazolium sidechain, indicating the presence of multiple conformations.

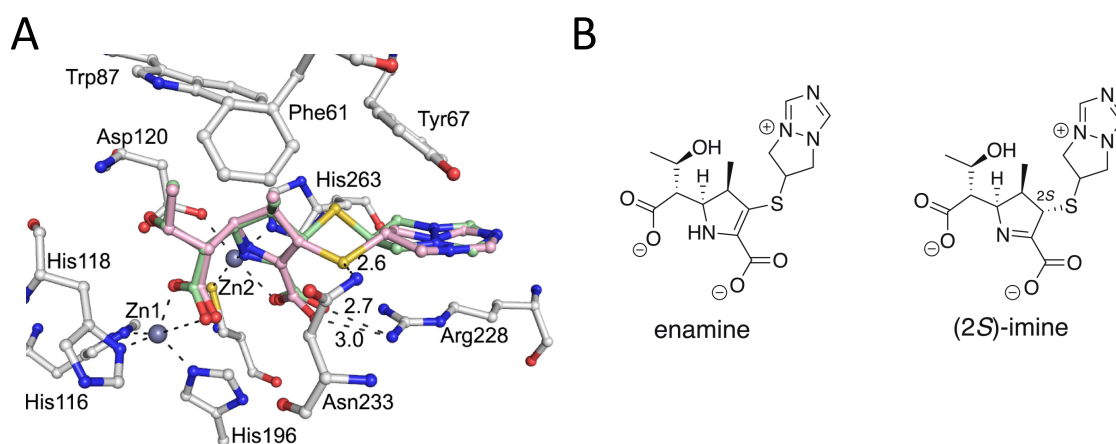


Figure 4. Views of a crystal structure of VIM-2 complexed with biapenem-derived ligands (PDB 6Y6J). (A) Interactions occurring between the (2*S*)-imine (green) and enamine (pink) products at the VIM-2 active site. Note that both products interact via their C3 carboxylate with Arg228 and that the sulfur of the thioether sidechain of the enamine is positioned adjacent to the primary amide of Asn233. (B) The (2*S*)-imine and enamine tautomers were each modelled at 50% occupancy.

When compared with a VIM-1: meropenem-derived (2*S*)-imine structure (PDB: 5N5I) [19], the binding modes in the VIM-2: biapenem-derived complex structure manifest some differences (Figure S7). The C6 hydroxyethyl group and newly formed carboxylate in the VIM-1: meropenem (2*S*)-imine product complex structure [19] have different orientations compared to VIM-2: biapenem products complex for both the enamine and the (2*S*)-imine. Notably, the binding modes of the VIM-2: biapenem-derived ligand complex and the VIM-2: faropenem Z-alkene imine-derived ligand complex appear more similar, with the analogous positioning of the C2 carboxylate (Figures S7 and S8) [20]. There are also differences in the binding modes of biapenem derived ligands when reacted with penicillin binding proteins and the class B2 MBL CphA (Figure S8). It is also notable that the different tautomeric complexes formed by carbapenem-derived ligands with MBLs are mimicked to different extents by various heterocyclic MBL inhibitors binding at the di-Zn(II) containing active site, as observed by crystallography [28,29].

3. Discussion

Previous studies have shown that the SBL/MBL catalysis of carbapenem hydrolysis results in the formation of enamine and (2*R*) and or (2*S*)-imines as the major observed hydrolysed products observed in the NMR analyses, with the analogous β -lactones being additionally observed in the case of class D SBLs [7–9,11]. Consistent with these findings, in the results reported here with biapenem, the (2*S*)-imine was observed as the major product with the B1 metallo- β -lactamases VIM-1, VIM-2 and the class A serine- β -lactamase KPC-2, at least on the relatively long timescale of the NMR assays. This observation indicates that the unusual biapenem bicyclo[3.2.1]hept-2-ylidene side chain does not substantially perturb the enamine/imine equilibrium position in the product enamine and imine tautomers (Figures 2 and S1–S4).

We appreciate that care should be taken in assigning crystallographically observed complexes, at least in terms of the details of binding, as being relevant to catalytically relevant intermediate structures in solution. However, consistent with the solution studies employing NMR, the crystallographic analysis of VIM-2 crystals soaked with biapenem revealed evidence for the enamine and the (2*S*)-imine as the major products bound, with no evidence for the (2*R*)-imine. We cannot rule out that the (2*R*)-imine, along with other ligands, may be formed at the active site at low levels, either in crystallo or in solution. In solution, at least for some carbapenems, the (2*R*)-imine is the kinetic product of enamine tautomerisation [7,9,10]. Thus, it is possible that we did not observe the (2*R*)-imine in part because of the relatively long timescale of the crystallographic analyses, which involved a 10 min crystal-soaking procedure. However, our combined results are also consistent with the proposal that during efficient catalysis, the enamine might be the major nascent product, with subsequent optimisation to the (2*R*)-imine and then (2*S*)-imines occurring in solution [7,9]. The formation of the (2*S*)-imine and, maybe, (2*R*)-imine can also occur at the active site in crystallo, at least as observed for the (2*S*)-imine in our VIM-2: biapenem work and with previous VIM-1: meropenem work [19].

Detailed spectroscopic analyses are required, both in solution and in crystals, to understand the precise nature of the reactions, including tautomerisations, that carbapenems undergo when bound to SBL and MBL active sites. It should also be noted that the observed product ratios are dependent on the efficiency of β -lactamase catalysis relative to that of tautomerisation, either in solution or in crystallo. Nonetheless, the combined results suggest that work aiming to prolong the lifetimes of the β -lactamase-bound carbapenem products is of interest with respect to developing improved carbapenems. This might be achieved either by the modification of the C2 carbapenem side chain or other group, in order to optimise the tautomerisation of the bound enamine tautomer to the (2*R*)-imine and potentially more stable (2*S*)-imine tautomer. The combined mechanistic studies with current clinically used carbapenems, including biapenem, however, suggest that the synthesis of new types of carbapenems may be required to achieve this.

4. Materials and Methods

4.1. Protein Purification and X-ray Crystallography

Recombinant forms of VIM-1, VIM-2, and KPC-2 were purified to near homogeneity (by SDS-PAGE analysis), as described [20,30,31]. VIM-2 (8.5 mg/mL) was crystallised using the vapour diffusion method under previously described conditions (Art Robbins low profile 96 well Intelli-plates) [20,30,31]. Crystallisation plates were set up using a PhoenixRE (ArtRobbins, Sunnyvale, CA, USA) robot with droplets of volume 200–300 nL with a 1:1, 1:2, and 2:1 protein: reservoir ratio equilibrated against 80 μ L reservoir solution. VIM-2 crystals appeared after 24–48 h and were soaked with \sim 200–300 nL of 50 mM biapenem aqueous stock solution for 10 min. The crystal was harvested, then cryo-cooled using liquid nitrogen and sent for data collection at the Diamond Light Source.

4.2. Data Collection and Processing

Diffraction data were collected on a single crystal at 100K at Diamond Light Source beamline I04-1. Images were indexed and integrated using FastDP [32]; the structure was solved by molecular replacement with Phaser using a previously reported VIM-2 structure as a model (PDB file 4BZ3) [30,31,33,34]. A dataset was collected on a crystal soaked with biapenem for 10 min. After the first round of refinement, the $mF_o - DF_c$ map was consistent with the presence of (a) biapenem-derived ligand(s). The ligand was manually fitted using WinCOOT before the second round of refinement. Subsequent refinements were carried out using the program Phenix, with manual model building in WinCOOT [35–37]. After further refinement, the electron density maps implied the presence of two different imposed products. Trial refinements with the (2*S*)-imine, the (2*R*)-imine, or the enamine (independently); the two imines together at 50% occupancy; and the enamine with either the (2*S*)- or (2*R*)-imine at 50% occupancy were carried out. The best fit was obtained with the (2*S*)-imine and the enamine with 50% occupancy. The geometry restraints for the biapenem (2*S*)-imine and enamine-derived products were calculated using electronic ligand builder and optimisation workbench (eLBOW), and the electron density maps were calculated using PHENIX [35].

4.3. ¹H NMR Studies

NMR-monitored assays were performed with VIM-1 (0.28 μ M, final concentration) VIM-2 (0.28 μ M), and KPC-2 (0.28 μ M) mixed with 5 mM of biapenem in a 50 mM sodium phosphate solution at pH 7.6 with 10% (*v/v*) D₂O, using trimethylsilylpropanoic acid as an internal standard (2 μ L of a 3 mg/mL solution). Experiments were conducted using a Bruker AVIIIHD 600 MHz spectrometer equipped with a Prodigy broadband cryoprobe. Water signal suppression was conducted using excitation sculpting with perfect echo. Chemical shift assignments were based on reported values; data were processed using MestReNova [38]. Time-courses are presented with earliest time point at the bottom and last time point (40 min) at the top (Figure 2 and Figures S1–S3). The spectrum of biapenem (5 mM) is displayed at the bottom. Each spectrum was acquired at 2.5 min intervals (16 scans). Note that the presence of the enamine product was assigned based on previous studies.

Supplementary Materials: The following supporting information can be downloaded at <https://www.mdpi.com/article/10.3390/antibiotics11030396/s1>. Table S1. Chemical shift assignments for the major biapenem-derived hydrolysis product. The chemical shifts and the C2 coupling constants (*J* 3.6, 1.3 Hz) of this hydrolysis product suggest that it is likely the (2*S*)-imine based on previous studies [8,9]; Table S2. Data collection and refinement statistics. High resolution statistics (1.36–1.33) are in parentheses. Due to poor completeness, the resolution for data processing was cut of to 1.5 Å, with a high resolution shell of 1.556–1.5 Å; Figure S1. ¹H NMR time course analysis of methyl group resonances of species formed on reaction of biapenem with KPC-2. Biapenem (5 mM, green) was treated with KPC-2 (280 nM) in 50 mM sodium phosphate at pH 7.5, 10% (*v/v*) D₂O. Evidence was accrued for formation of (2*R*)-imine, (2*S*)-imine and enamine products (blue, purple,

and pink, respectively). 15 spectra were acquired (16 scans, every 2.5 min) over 37.5 min (stacked from bottom/first spectrum to top). The bottom spectrum is of biapenem (5 mM) without added enzyme; Figure S2. ^1H NMR time course analysis of methyl group resonances of species formed on reaction of biapenem with VIM-1. Biapenem (5 mM, green) was treated with VIM-1 (280 nM) in 50 mM sodium phosphate at pH 7.5, 10% (*v/v*) D_2O . Unassigned product peaks are labelled with asterisks. Evidence was accrued for formation of (2*R*)-imine, (2*S*)-imine and enamine products (blue, purple, and pink, respectively). 15 spectra were acquired (16 scans, every 2.5 min) over 37.5 min (stacked from bottom/first spectrum to top). The bottom spectrum is biapenem (5 mM) without added enzyme; Figure S3. ^1H NMR time course analysis of methyl group resonances of products formed on reaction of biapenem with VIM-2. Biapenem (5 mM, green) was treated with VIM-2 (280 nM) in 50 mM sodium phosphate at pH 7.5, 10% (*v/v*) D_2O . Evidence was accrued for formation of (2*R*)-imine and (2*S*)-imine and enamine products (blue, purple, and pink, respectively). 8 spectra were acquired (16 scans, every 2.5 min) over 20 min (stacked from bottom/first spectrum to top). The bottom spectrum is biapenem (5 mM) without added enzyme; Figure S4. ^1H -NMR time course analyses for reaction of biapenem with VIM-1 and VIM-2 (MBLs) and KPC-2 (an SBL). Methyl group resonance peak integrations from time course data were analysed to monitor reaction of biapenem to give (2*R*)-imine, (2*S*)-imine and enamine (blue, pink, and purple, respectively) products using a Bruker AVIIIHD 600 MHz machine. Biapenem (5 mM) was treated with (A) VIM-1 (280 nM), (B) VIM-2 (280 nM), (C) KPC-2 (280 nM) and (D) VIM-2 (100 nM) in 50 mM sodium phosphate at pH 7.5, 10% (*v/v*) D_2O . Integration of methyl resonance of biapenem was normalised ((integration of biapenem) / (integration of biapenem + (2*R*)-imine + (2*S*)-imine + enamine) \times 100) was used to calculate the percentage of biapenem turnover; Figure S5. View of the overall fold of the VIM-2: biapenem derived complex. (A) The structure was processed in the space group *I*222 (PDB 6Y6J). Zinc ions are shown as grey spheres and chloride ions are in green. (B) Active site view of VIM-2 complexed with biapenem derived products. Relevant loops for interaction are labelled. The biapenem derived enamine ligand is in pale pink, and the biapenem derived imine ligand is in pale green (Figure S6); Figure S6. (A) Interactions between the biapenem derived enamine ligand (3) and the VIM-2 active site. (B) Interactions between the biapenem derived (2*S*)-imine (1) derived ligand and the VIM-2 active site; Figure S7. Comparisons of conformations of carbapenem and penem derived ligands with VIM-1 and VIM-2. (A) View of VIM-1 complexed with (i) the meropenem derived (2*S*)-imine ligand in slate blue (PDB 5N5I [19]); (ii) the VIM-2 biapenem derived (2*S*)-imine in green; and (iii) the VIM-2 biapenem derived enamine in pink. (PDBs: 6Y6J). (B) View of VIM-2 complexed with the (i) faropenem derived product (purple) (PDBs: 7A5Z [20]); (ii) the biapenem derived (2*S*)-imine in green and (iii) the biapenem derived enamine in pink. (PDBs: 6Y6J). Note that the binding modes of the faropenem derived imine (*Z*)-alkene (dark purple) and biapenem (2*S*)-imine derived ligands are similar; Figure S8. Overlay of the conformations of biapenem derived enamine and imine ligands with β -lactamases and penicillin binding proteins. Colour code: VIM-2 (class B1 MBL) complexed with the biapenem derived enamine—light pink; VIM-2 complexed with the biapenem derived (2*S*)-imine—light green (PDB 6Y6J); PBP2X complexed with the biapenem derived enamine—slate blue (PDB 2ZC3), PBP1A complexed with the biapenem substrate—orange (PDB 2ZC5) [24], and CphA (class B2 MBL) complexed with the biapenem derived enamine—purple (PDB 1X8I) [23].

Author Contributions: Conceptualisation, J.B. and C.J.S.; methodology, A.L.; provision of materials, C.L.T., K.C. and T.R.M.; formal analysis, A.L., M.A.M. and T.R.M.; investigation, C.J.S. and J.S.; data curation, A.L.—original draft preparation, A.L.; writing, analysis, review, and editing, A.L. and C.J.S.; project administration, C.J.S.; funding acquisition, C.J.S. and J.S. All authors have read and agreed to the published version of the manuscript.

Funding: We thank the Medical Research Council (EP/L016044/1, MR/T016035/1), the Biotechnology and Biological Research Council (BB/S50676X/1), and the Ineos Oxford Institute for Antimicrobial Research for funding. T.R.M. was supported by the BBSRC (BB/M011224/1). This research was funded in whole, or in part, by the Wellcome Trust (grant no. 106244/Z/14/Z and no. 099141/Z/12/Z).

Institutional Review Board Statement: Not applicable.

Informed Consent Statement: Not applicable.

Data Availability Statement: PDB available at <https://www.rcsb.org/structure/6Y6J> (accessed on 20 January 2022).

Acknowledgments: We thank the beamline scientists at the Diamond Light Source and the NMR team at the Chemistry Research Laboratory for their technical support.

Conflicts of Interest: The authors declare no conflict of interest.

References

1. Bush, K.; Bradford, P.A. β -Lactams and β -Lactamase Inhibitors: An Overview. *Cold Spring Harb. Perspect. Med.* **2016**, *6*, 1–22. [[CrossRef](#)] [[PubMed](#)]
2. Fair, R.J.; Tor, Y. Antibiotics and Bacterial Resistance in the 21st Century. *Perspect. Med. Chem.* **2014**, *6*, 25–64. [[CrossRef](#)] [[PubMed](#)]
3. Bush, K. Bench-to-Bedside Review: The Role of Beta-Lactamases in Antibiotic-Resistant Gram-Negative Infections. *Crit. Care.* **2010**, *14*, 1–8. [[CrossRef](#)] [[PubMed](#)]
4. Bush, K. Metallo-Beta-Lactamases: A Class Apart. *Clin. Infect. Dis.* **1998**, *27*, S48–S53. [[CrossRef](#)]
5. Paterson, D.L.; Bonomo, R.A. Extended-Spectrum β -Lactamases: A Clinical Update. *Clin. Microbiol. Rev.* **2005**, *18*, 657–686. [[CrossRef](#)] [[PubMed](#)]
6. Meini, M.-R.; Llarrull, L.I.; Vila, A.J. Evolution of Metallo- β -lactamases: Trends Revealed by Natural Diversity and in vitro Evolution. *Antibiotics* **2014**, *3*, 285–316. [[CrossRef](#)] [[PubMed](#)]
7. Lohans, C.T.; Van Groesen, E.; Kumar, K.; Tooke, C.L.; Spencer, J.; Paton, R.S.; Brem, J.; Schofield, C.J. A New Mechanism for β -Lactamases: Class D Enzymes Degrade 1 β -Methyl Carbapenems through Lactone Formation. *Angew. Chem.* **2018**, *130*, 1296–1299. [[CrossRef](#)]
8. Aertker, K.M.J.; Chan, H.T.H.; Lohans, C.T.; Schofield, C.J. Analysis of β -Lactone Formation by Clinically Observed Carbapenemases Informs on a Novel Antibiotic Resistance Mechanism. *J. Biol. Chem.* **2020**, *295*, 16604–16613. [[CrossRef](#)] [[PubMed](#)]
9. Lohans, C.T.; Freeman, E.I.; van Groesen, E.; Tooke, C.L.; Hinchliffe, P.; Spencer, J.; Brem, J.; Schofield, C.J. Mechanistic Insights into β -Lactamase-Catalysed Carbapenem Degradation Through Product Characterisation. *Sci. Rep.* **2019**, *9*, 1–9. [[CrossRef](#)]
10. van Groesen, E.; Lohans, C.T.; Brem, J.; Aertker, K.M.; Claridge, T.D.W.; Schofield, C.J. 19F-NMR Monitoring of Reversible Protein Post-Translational Modifications: Class D β -Lactamase Carbamylation and Inhibition. *Chem. Eur. J.* **2019**, *25*, 11837–11841. [[CrossRef](#)] [[PubMed](#)]
11. Lisa, M.-N.; Palacios, A.R.; Aitha, M.; González, M.M.; Moreno, D.M.; Crowder, M.W.; Bonomo, R.A.; Spencer, J.; Tierney, D.L.; Llarrull, L.I.; et al. A General Reaction Mechanism for Carbapenem Hydrolysis by Mononuclear and Binuclear Metallo- β -Lactamases. *Nat. Comm.* **2017**, *8*, 538. [[CrossRef](#)] [[PubMed](#)]
12. Bonfiglio, G.; Maccarone, G.; Mezzatesta, M.L.; Privitera, A.; Carciotto, V.; Santagati, M.; Stefani, S.; Nicoletti, G. In vitro Activity of Biapenem against Recent Gram-Negative and Gram-Positive Clinical Isolates. *Chemotherapy* **1997**, *43*, 393–399. [[CrossRef](#)] [[PubMed](#)]
13. Kumagai, T.; Tamai, S.; Abe, T.; Matsunaga, H.; Hayashi, K.; Kishi, I.; Shiro, M.; Nagao, Y. New Straightforward Synthesis and Characterization of a Unique 1 β -Methylcarbapenem Antibiotic Biapenem Bearing a σ -Symmetric Bicyclo[3.2.1]octane Group as the Pendant Moiety. *J. Org. Chem.* **1998**, *63*, 8145–8149. [[CrossRef](#)]
14. Perry, C.M.; Ibbotson, T. Biapenem. *Drugs* **2002**, *62*, 2221–2234. [[CrossRef](#)] [[PubMed](#)]
15. Lepsanovic, Z.; Libisch, B.; Tomanovic, B.; Nonkovic, Z.; Balogh, B.; Füzi, M. Characterisation of the First VIM Metallo- β -Lactamase-Producing *Pseudomonas Aeruginosa* Clinical Isolate in Serbia. *Acta Microbiol. Immunol. Hung.* **2008**, *55*, 447–454. [[CrossRef](#)] [[PubMed](#)]
16. Mavroidi, A.; Tsakris, A.; Tzelepi, E.; Pournaras, S.; Loukova, V.; Tzouveleki, L.S. Carbapenem-hydrolysing VIM-2 metallo-beta-lactamase in *Pseudomonas aeruginosa* from Greece. *J. Antimicrob. Chemother.* **2000**, *46*, 1041–1043. [[CrossRef](#)]
17. Docquier, J.-D.; Lamotte-Brasseur, J.; Galleni, M.; Amicosante, G.; Frère, J.-M.; Rossolini, G.M. On functional and structural heterogeneity of VIM-type metallo-beta-lactamases. *J. Antimicrob. Chemother.* **2003**, *51*, 257–266. [[CrossRef](#)]
18. Makena, A.; Düzgün, A.Ö.; Brem, J.; McDonough, M.A.; Rydzik, A.M.; Abboud, M.I.; Saral, A.; Çiçek, Ç.A.; Sandalli, C.; Schofield, C.J. Comparison of Verona Integron-Borne Metallo-Lactamase (VIM) Variants Reveals Differences in Stability and Inhibition Profiles. *Antimicrob. Agents Chemother.* **2016**, *60*, 1377–1384. [[CrossRef](#)]
19. Salimraj, R.; Hinchliffe, P.; Kosmopoulou, M.; Tyrrell, J.M.; Brem, J.; van Berkel, S.S.; Verma, A.; Owens, R.J.; McDonough, M.A.; Walsh, T.R.; et al. Crystal Structures of VIM-1 Complexes Explain Active Site Heterogeneity in VIM-Class Metallo- β -Lactamases. *FEBS J.* **2019**, *286*, 169–183. [[CrossRef](#)] [[PubMed](#)]
20. Lucic, A.; Hinchliffe, P.; Malla, T.R.; Tooke, C.L.; Brem, J.; Calvopiña, K.; Lohans, C.T.; Rabe, P.; McDonough, M.A.; Armistead, T.; et al. Faropenem Reacts with Serine and Metallo- β -Lactamases to Give Multiple Products. *Eur. J. Med. Chem.* **2021**, *215*, 1–10. [[CrossRef](#)]
21. Mehta, S.C.; Furey, I.M.; Pemberton, O.A.; Boragine, D.M.; Chen, Y.; Palzkill, T. KPC-2 β -lactamase enables carbapenem antibiotic resistance through fast deacylation of the covalent intermediate. *J. Biol. Chem.* **2021**, *296*, 1–15. [[CrossRef](#)] [[PubMed](#)]
22. Galdadas, I.; Lovera, S.; Pérez-Hernández, G.; Barnes, M.D.; Healy, J.; Afsharikh, H.; Woodford, N.; Bonomo, R.A.; Gervasio, F.L.; Haider, S. Defining the Architecture of KPC-2 Carbapenemase: Identifying Allosteric Networks to Fight Antibiotics Resistance. *Sci. Rep.* **2018**, *8*, 1–13. [[CrossRef](#)]

23. Garau, G.; Bebrone, C.; Anne, C.; Galleni, M.; Frère, J.-M.; Dideberg, O. A Metallo- β -lactamase Enzyme in Action: Crystal Structures of the Monozinc Carbapenemase CphA and its Complex with Biapenem. *J. Mol. Biol.* **2005**, *345*, 785–795. [[CrossRef](#)] [[PubMed](#)]
24. Yamada, M.; Watanabe, T.; Baba, N.; Takeuchi, Y.; Ohsawa, F.; Gomi, S. Crystal Structures of Biapenem and Tebipenem Complexed with Penicillin-Binding Proteins 2X and 1A from *Streptococcus Pneumoniae*. *Antimicrob. Agents Chemother.* **2008**, *52*, 2053–2060. [[CrossRef](#)] [[PubMed](#)]
25. Bianchet, M.A.; Pan, Y.H.; Basta, L.A.B.; Saavedra, H.; Lloyd, E.P.; Kumar, P.; Mattoo, R.; Townsend, C.A.; Lamichhane, G. Structural insight into the inactivation of Mycobacterium tuberculosis non-classical transpeptidase LdtMt2 by biapenem and tebipenem. *BMC Biochem.* **2017**, *18*, 1–14. [[CrossRef](#)] [[PubMed](#)]
26. Yamaguchi, Y.; Jin, W.; Matsunaga, K.; Ikemizu, S.; Yamagata, Y.; Wachino, J.; Shibata, N.; Arakawa, Y.; Kurosaki, H. Crystallographic Investigation of the Inhibition Mode of a VIM-2 Metallo- β -Lactamase from *Pseudomonas Aeruginosa* by a Mercaptocarboxylate Inhibitor. *J. Med. Chem.* **2007**, *50*, 6647–6653. [[CrossRef](#)] [[PubMed](#)]
27. Tooke, C.L.; Hinchliffe, P.; Bragginton, E.C.; Colenso, C.K.; Hirvonen, V.H.A.; Takebayashi, Y.; Spencer, J. β -Lactamases and β -Lactamase Inhibitors in the 21st Century. *J. Mol. Biol.* **2019**, *431*, 3472–3500. [[CrossRef](#)] [[PubMed](#)]
28. Brem, J.; Panduwawala, T.; Hansen, J.U.; Hewitt, J.; Liepins, E.; Donets, P.; Espina, L.; Farley, A.J.M.; Shubin, K.; Campillos, G.G.; et al. Imitation of β -lactam binding enables broad-spectrum metallo- β -lactamase inhibitors. *Nat. Chem.* **2022**, *14*, 15–24. [[CrossRef](#)]
29. Davies, D.T.; Leiris, S.; Sprynski, N.; Castandet, J.; Lozano, C.; Bousquet, J.; Zalacain, M.; Vasa, S.; Dasari, P.K.; Pattipati, R.; et al. ANT2681: SAR Studies Leading to the Identification of a Metallo- β -Lactamase Inhibitor with Potential for Clinical Use in Combination with Meropenem for the Treatment of Infections Caused by NDM-Producing *Enterobacteriaceae*. *ACS Infect. Dis.* **2020**, *6*, 2419–2430. [[CrossRef](#)]
30. Cahill, S.; Tarhonskaya, H.; Rydzik, A.; Flashman, E.; McDonough, M.A.; Schofield, C.J.; Brem, J. Use of ferrous iron by metallo- β -lactamases. *J. Inorg. Biochem.* **2016**, *163*, 185–193. [[CrossRef](#)] [[PubMed](#)]
31. Parkova, A.; Lucic, A.; Krajnc, A.; Brem, J.; Calvopiña, K.; Langley, G.W.; McDonough, M.A.; Trapencieris, P.; Schofield, C.J. Broad Spectrum β -Lactamase Inhibition by a Thioether Substituted Bicyclic Boronate. *ACS Infect. Dis.* **2020**, *6*, 1398–1404. [[CrossRef](#)] [[PubMed](#)]
32. Winter, G.; Waterman, D.G.; Parkhurst, J.M.; Brewster, A.S.; Gildea, R.J.; Gerstel, M.; Fuentes-Montero, L.; Vollmar, M.; Michels-Clark, T.; Young, I.; et al. DIALS: Implementation and evaluation of a new integration package. *Acta Crystallogr. Sect. D Struct. Biol.* **2018**, *74*, 85–97. [[CrossRef](#)] [[PubMed](#)]
33. Brem, J.; van Berkel, S.S.; Zollman, D.; Lee, S.Y.; Gileadi, O.; McHugh, P.J.; Walsh, T.R.; McDonough, M.A.; Schofield, C.J. Structural Basis of Metallo- β -Lactamase Inhibition by Captopril Stereoisomers. *Antimicrob. Agents Chemother.* **2016**, *60*, 142–150. [[CrossRef](#)] [[PubMed](#)]
34. McCoy, A.J.; Grosse-Kunstleve, R.W.; Adams, P.D.; Winn, M.D.; Storoni, L.C.; Read, R.J. Phaser Crystallographic Software. *J. App. Crystallogr.* **2007**, *40*, 658–674. [[CrossRef](#)]
35. Adams, P.D.; Afonine, P.V.; Bunkóczi, G.; Chen, V.B.; Davis, I.W.; Echols, N.; Headd, J.J.; Hung, L.-W.; Kapral, G.J.; Grosse-Kunstleve, R.W.; et al. PHENIX: A Comprehensive Python-Based System for Macromolecular Structure Solution. *Acta Crystallogr. D. Biol. Crystallogr.* **2010**, *66*, 213–221. [[CrossRef](#)]
36. Afonine, P.V.; Grosse-Kunstleve, R.W.; Echols, N.; Headd, J.J.; Moriarty, N.W.; Mustyakimov, M.; Terwilliger, T.C.; Urzhumtsev, A.; Zwart, P.H.; Adams, P.D. Towards automated crystallographic structure refinement with phenix.refine. *Acta Crystallogr. Sect. D Biol. Crystallogr.* **2012**, *68*, 352–367. [[CrossRef](#)]
37. Emsley, P.; Cowtan, K. Coot: Model-building tools for molecular graphics. *Acta Crystallogr. Sect. D Struct. Biol.* **2004**, *D60*, 2126–2132. [[CrossRef](#)]
38. Willcott, M.R. MestRe Nova. *J. Am. Chem. Soc.* **2009**, *131*, 13180. [[CrossRef](#)]